

Combined passive and active ultrasonic stress wave monitoring of UHPFRC properties on a structural level

Numa Bertola, Ph.D. (corresponding author) – Postdoctoral Researcher, Laboratory for Maintenance and Safety of Structures, Swiss Federal Institute of Technology (EPFL), Lausanne, Switzerland, Email: numa.bertola@epfl.ch

Thomas Schumacher, Ph.D. – Associate Professor, Civil and Environmental Engineering, Portland State University; Portland, OR, USA.

Ernst Niederleithinger, Ph.D. – Head of Non-destructive Testing Methods for Civil Engineering, Bundesanstalt für Materialforschung und -prüfung, Berlin, Germany.

Eugen Brühwiler, Ph.D. – Full Professor, Laboratory for Maintenance and Safety of Structures, Swiss Federal Institute of Technology (EPFL), Lausanne, Switzerland.

Abstract

Ultra-High-Performance Fiber-Reinforced Cementitious Composite (UHPFRC) is becoming popular in designing lightweight and durable structures. UHPFRC structural elements remain crack-free and waterproof under service conditions, significantly improving durability compared to designs made of conventional reinforced concrete. Due to its unique composition, UHPFRC has specific mechanical properties. In particular, the early-age development of UHPFRC properties, such as the elastic modulus, is difficult to monitor as it occurs while elements are in the formwork. Monitoring of the very early-age behavior of UHPFRC is thus challenging, which is why the hydration process of UHPFRC on a structural level is still not yet fully understood. This paper proposes a novel combined passive and active ultrasonic stress wave monitoring (USW) approach involving a network of ultrasonic transducers and thermocouples. The scheme was applied to a laboratory beam with a span length of 4.0 meters. The monitoring network consisted of 24 embedded ultrasonic transducers and 15 thermocouples and allowed data recording from the beginning of the UHPFRC hardening process. From the beginning, a set of ultrasonic pulses were emitted every 30 minutes and recorded (active USW monitoring), while acoustic emissions (AE) were recorded continuously (passive USW monitoring). After 28 days, the beam was moved into a load frame and tested under four-point bending. Continuous monitoring using this unique passive and active monitoring approach enabled accurate characterization of the evolution of material properties during the very early age of UHPFRC, as well as the structural behavior and degradation processes of the beam during structural load testing.

Keywords: Ultra-High-Performance Fibre Reinforced Cementitious Composite; Acoustic emission monitoring; Ultrasonic stress wave monitoring; Embedded ultrasonic transducers; Experimental laboratory testing; Early-age properties.

1. Introduction

Ultra-High-Performance Fibre-Reinforced Cementitious Composite (UHPFRC) is one of the most durable cementitious materials. UHPFRC is made of a paste with a high cement content, fine-hard particles (i.e. sand and silica fume with a maximum grain size of 1 mm), water (water/binder ratio of 0.15-0.2), additives, superplasticizer, and short slender steel fibers (Brühwiler and Denarié). These fibers typically account for 3% of the UHPFRC volume. Over the last twenty years, there have been several hundred applications of this material in bridge engineering, both for new designs and structural rehabilitation (Graybeal et al.; Bertola, Schiltz, et al.).

The 28-day mechanical properties of UHPFRC are summarized in (Brühwiler). Maximum values of the tensile and compressive strengths are up to 16 and 200 MPa, respectively. The modulus of elasticity is approximately 45 GPa, and the material exhibits strain-hardening behavior in tension up to a deformation of 1-2%. The tensile strength can be increased further by adding reinforcement bars (R-UHPFRC), analogous to reinforced concrete (RC) structures. In 2016, the Swiss Technical Leaflet on UHPFRC was released (SIA 2052) for the design of UHPFRC structures and the strengthening of existing RC elements (*Technical Leaflet on UHPFRC: Materials, Design and Application*).

Researchers have also investigated the development of mechanical properties with respect to the UHPFRC age. Tensile and compressive strengths and the elastic modulus have been shown to develop much faster compared to conventional concrete (Habel et al.). Due to its low water/binder ratio, the hydration process of UHPFRC has been studied. The hydration degree is between 30 and 50% at 28 days, which is significantly lower compared to conventional concrete (Habel and Gauvreau). It has also been found that the capillary water depletes quickly, and the hydration process continues using gel water (Kazemi-Kamyab et al.).

The monitoring approach discussed herein involves the implementation of a unique sensor network composed of embedded ultrasonic transducers [Model ACS S0807 (Niederleithinger et al.)] that are capable of both recording acoustic emissions (passive monitoring) as well as emitting consistent ultrasonic pulses, allowing active monitoring (Schumacher and Niederleithinger). 24 transducers, as well as 15 thermocouples, were embedded in a 4.2-meter-long beam made of UHPFRC. In the first phase, this monitoring system aimed to capture the development of the early-age UHPFRC properties. During the four-point bending load test, the monitoring systems aimed at quantifying degradation processes and load levels throughout test duration.

2. Monitoring setup

A UHPFRC T-shape beam with a length of 4200 mm and a depth of 400 mm was cast at the EPFL laboratory facility with an embedded sensor network involving 24 ultrasonic transducers and 15 thermocouples distributed within the beam's web (Figure 1). The goals of this study were to monitor (a) the development of early-age UHPFRC properties while the specimen remained in the formwork and (b) degradation processes during load testing 28 days after casting using both passive (AE) and active USW.

The UHPFRC mix used in this specimen involves 3.4 vol-% of short and slender steel fibers (length of 13 mm and diameter of 0.16 mm). The commercial premix is composed of cement, silica fume, and sand. The water/binder ratio was 0.18 and 3.4% additive (superplasticizer) was added.

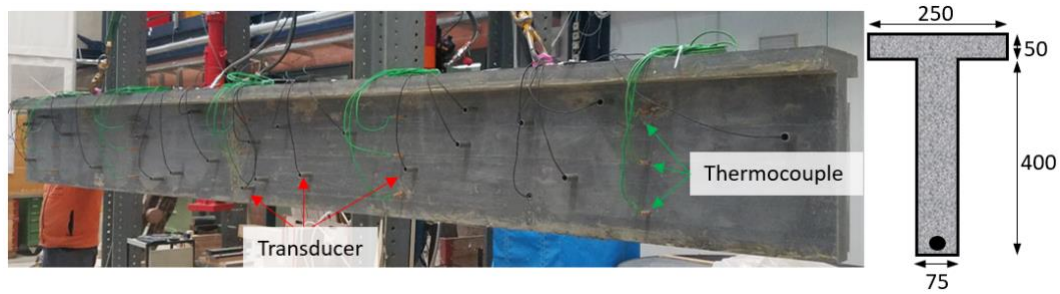


Figure 1 Monitoring setup for the 4.2-meter beam to measure the early-age properties of UHPFRC involving both passive and active USW monitoring with distributed sensor network in the beam web: Photo (left) and cross-section (right) of the beam.

3. Early-age monitoring (Phase 1)

3.1. Introduction

Data collection of the early-age UHPFRC started 2,7 hours after casting and lasted for 20 days. The reported age is relative to the time when water was added to the UHPFRC premix, which is when cement hydration was initiated. During the entire monitoring phase, the beam remained in its formwork and was placed in a quiet area of the laboratory. For both passive and active USW monitoring, a Vallen AMSY-6 system was used, which has the ability to produce consistent pulses for the active monitoring part.

During active monitoring, each transducer was sequentially used as the pulsing device, and the remaining transducers recorded the response. Four pulses were produced from the emitting transducer at a pulse repetition frequency of 1 Hz. The pulsing occurred every 30 minutes during the 20 days of monitoring. Passive monitoring involved capturing the AE with 24 transducers during the same duration.

3.2. Monitoring data

Both passive and active measurements are presented in this section. In active USW monitoring, a pulse is emitted by each transducer sequentially, and a recording is triggered by the other transducers, with the transient waveforms being stored for post-analysis and processing. From the network of 24 transducers, a total of 552 emitter-receiver couples were recorded. Several properties of these signals can then be analyzed. In this study, the P-wave velocity of the ultrasonic pulse is investigated.

The P-wave velocity is calculated as the ratio between the Euclidian distance of transducer couples and the P-wave travel time. The travel time requires precisely picking the P-wave arrival time, which can be challenging for low-amplitude and noisy waveforms. An automatic picker based on the Akaike Information Criterion (AIC) was used (Kurz et al.). The P-wave velocity for each transducer couple is shown in Figure 2 with respect to the UHPFRC age. Several transducer couples produced P-wave velocities outside the range obtained by the majority of couples. These data were defined as outliers and removed from the analysis. It can be observed that the P-wave velocity increases significantly during the first 40 hours and then remains almost constant after that time. Most couples measure a final stable P-wave velocity between 4200 and 5000 m/s (mean values of 4680 m/s, standard deviation of 170 m/s).

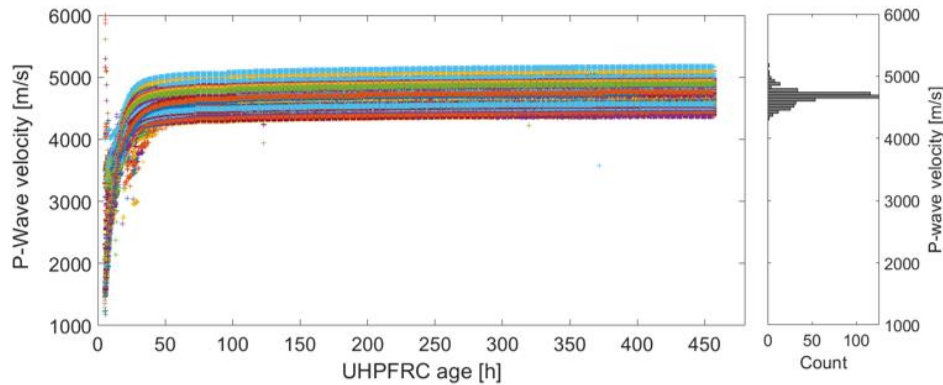


Figure 2 Estimated P-wave velocities vs. UHPFRC age for transducer couples after removing outliers.

The monitoring system also recorded AE (passive monitoring approach) during the early age of UHPFRC. AE are stress waves that result from a sudden release of energy within a material due to cracking. In this study, the micro-cracking response of the early-age UHPFRC is investigated.

Figure 3 presents AE rates vs. UHPFRC age. The AE rate significantly increases during the first 24 hours and remains high until about 200 hours. A change of phase is observed after 7 to 8 days.

AE hit rates with the mean temperature recorded can be compared to the autogenous shrinkage from (Hajiesmaeili and Denarié) with a similar material mix. Moving averages at 24 periods are taken in order to smooth datasets. The first peak of the AE rate that occurs around 30 hours corresponds to the maximum temperature recorded and the highest autogenous shrinkage rate. This measurement technique thus enables the identification of the setting of the shrinkage process.

(Kazemi-Kamyab et al.) found that two main regimes occur in the hydration process. The first one is dominated by the clinker hydration during the first seven days, while after that time the increase in bound water and strength comes from the reaction of the silica fume. The first seven days, or 168 hours, corresponds reasonably to the end of the high AE rate observed in this monitoring campaign. Thus, AE measurements could potentially identify the change of hydration regime between clinker and silica fume in UHPFRC.

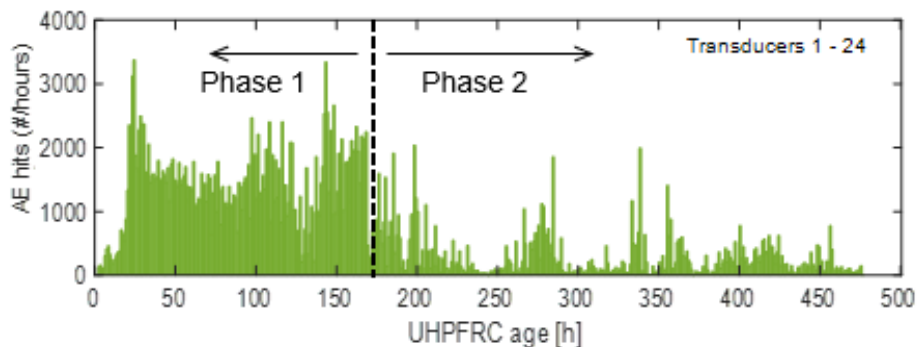


Figure 3 Hourly AE hits vs. UHPFRC age.

3.3. Inverse analysis – elastic modulus

In this section, the USW measurements are used to infer the development of the elastic modulus of UHPFRC. USW pulsing enables estimating the P-wave velocity between two actuators.

The P-wave velocity depends on three parameters of the material: dynamic modulus of elasticity, density, and Poisson's ratio, and is given by Equation (1). Based on the weight of the beam, which was determined using a calibrated load cell, the density was found to be, $\rho_U = 2600 \text{ kg/m}^3$. This value was assumed to be constant over the beam depth and length. (Kazemi Kamyab) showed that Poisson's ratio, ν of UHPFRC rapidly decreases from 0.5 to 0.2 during the first 24 hours, and this evolution was included in the estimates of the modulus of elasticity.

$$V_P = \sqrt{\frac{E_U}{\rho_U} * \frac{(1-\nu)}{(1+\nu)(1-2\nu)}} \quad (1)$$

The results of the inverse analysis are shown in Figure 4. Mean estimates, as well as 5% and 95% quantiles, of the dynamic modulus of elasticity are very close to values presented by the empirical study (Hajiesmaeili and Denarié). Although some variability of the estimates is observed (standard deviation of 2.5 GPa), This result validates that active USW monitoring can be used to infer the UHPFRC modulus of elasticity at an early age, while the UHPFRC element is still within the formwork.

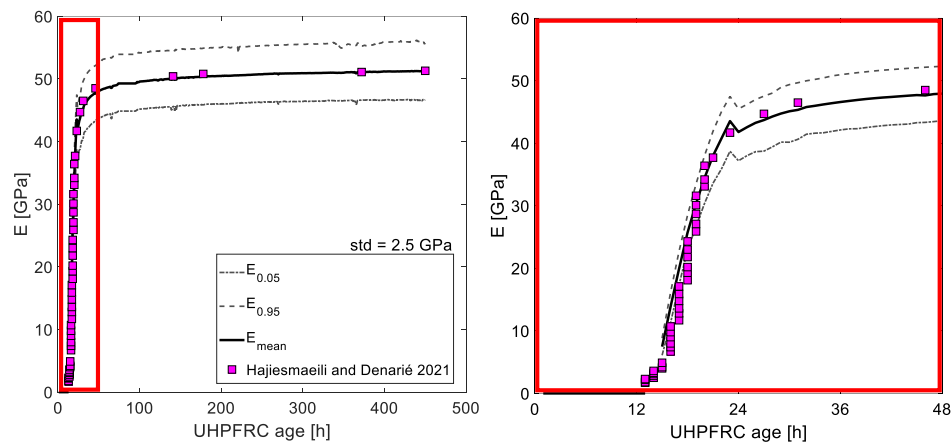


Figure 4 Development of UHPFRC dynamic modulus of elasticity vs. age.

4. Load testing (Phase 2)

4.1. Introduction

In the second phase of the monitoring, a four-point bending test is performed on the beam. The test setup is similar to (Bertola, Trinh, et al.). A traditional monitoring system (DIC, deflection measurement, and strain gauges) was installed in addition to the embedded transducer network. Several loading-unloading cycles were imposed at different load levels. Finally, the load was increased until the beam failed. A ductile failure was observed, and the failure crack appeared in the bending-only region of the beam (Figure 5).

AE (passive monitoring) were recorded throughout the test. USW (active monitoring) were emitted at each stage of the loading-unloading cycles and after failure. Again, four pulses were emitted by

each transducer at each load level. The combined monitoring approach was used to identify some of the most relevant properties of the beam behavior during load testing.

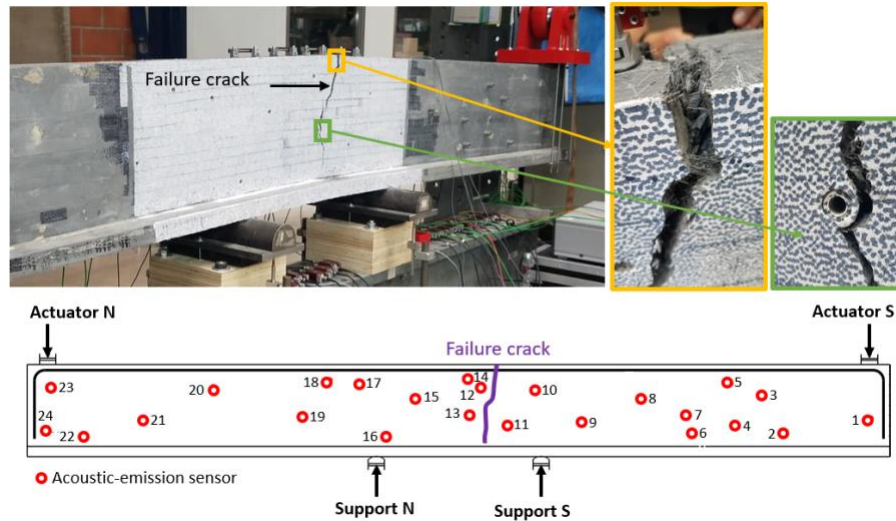


Figure 5 Photograph of the failure crack on the beam and location related to the transducer network.

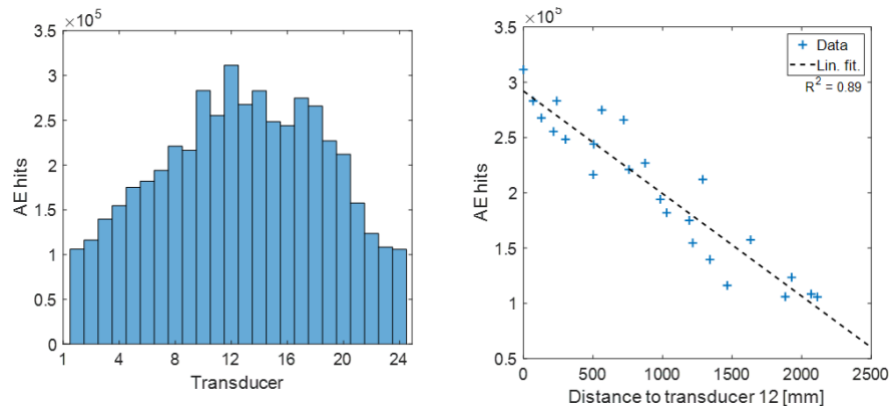


Figure 6 Left: recorded acoustic-emission (AE) per transducer; Right: relation of number of AE hits with distance to Transducer 12.

4.2 Crack location determination

First, recorded AE were used to infer the failure crack location. Figure 6 shows the AE hits recorded by each transducer individually. Transducer 12 recorded a significantly larger number of AE hits than other transducers. In addition, nearby transducers (i.e., # 10 and 14) also recorded significant AE activity. A strong correlation is observed between the number of AE hits and the distance to Transducer 12 (R^2 of 0.89). Therefore, it can be inferred that the failure crack developed in the beam web between Transducers 12 and 10. This result was confirmed by visual observation of the failure crack location (Figure 5).

This phase confirms that AE monitoring can help identify crack development in UHPFRC elements. Future work will extend these results to identify crack propagation within the beam depth.

4.3 Load level determination

Active USW monitoring was performed at the maximum and minimum load levels of the loading-unloading cycles. By comparing the P-wave velocities of the USW pulses during the loading-unloading cycles, it is possible to examine the behavior of the beam during load testing.

A few select transducer couples were analyzed throughout the loading process (Figure 7). After each loading-unloading cycle, P-wave velocity values were calculated for the minimum load level. Couple 1 and 2 is located near the South load application point (Figure 5), where the bending moment is small. For this couple, the beam property remains relatively unaffected throughout the load test. Therefore, this sensor can be used as a benchmark representing undamaged beam properties. P-wave velocity measurements of the remaining couples are relatively unaffected during the first three load-unloading cycles (13% of maximum load). Then, a significant drop can be observed that corresponds to the beginning of the non-linear behavior of UHPFRC. Moreover, transducer couple 10-12 has significant drops after the first loading-unloading cycle at 50% and 95% of the maximum load, respectively. These levels corresponded to when the failure crack was visible for the first time with the naked eye and its significant propagation in the beam web, respectively. By comparing transducer couples 10-12 and 12-15, which have similar distances, it is clear that crack propagation is responsible for this sudden drop in the P-wave velocity.

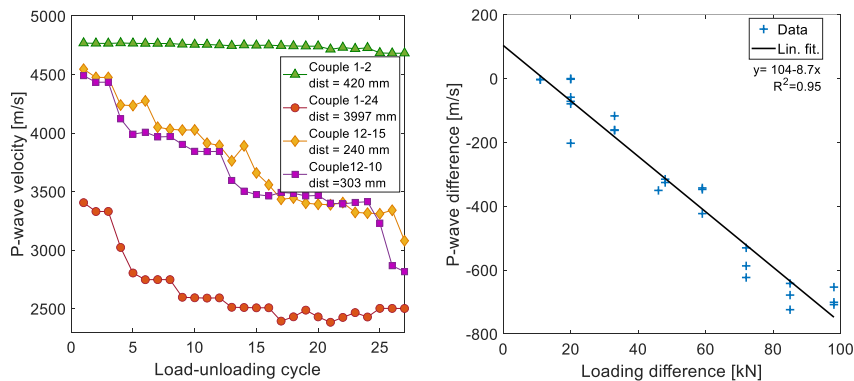


Figure 7 Left: evolution of the P-wave velocity with respect to the loading-unloading cycles for select transducer couples at the minimum load level; Right: relation between the load increase during cycles and increase of P-wave velocity for the transducer couple 1-23.

Another result is the relation between the P-wave velocity difference and the increase in loading. When using the transducer couple 1-24, which covers almost the entire length of the beam, it can be observed that the decrease of P-wave velocity during the unloading is directly proportional to the decrease of the load level ($R^2 = 0.95$). This observation shows that this monitoring technique can potentially be used for bridge weigh-in-motion (BWIM). Future work consists in confirming this result with additional transducer couples.

5. Conclusions

This study investigated a novel monitoring approach for capturing UHPFRC properties at an early age and during structural load testing. Instrumentation includes 24 embedded ultrasonic transducers in a 4.2-meter-long beam. Continuous monitoring using this novel passive (acoustic emission) and active USW monitoring approach enabled accurate characterization of the evolution of material properties, such as the elastic modulus during the very early age of UHPFRC, as well

Publication type: Full paper

Paper No: 22

as the structural behavior (load level) and degradation processes (crack location and propagation) of the beam during load testing. The presented approach offers new opportunities for holistic monitoring during the entire service period of a structure. Future work includes a detailed analysis of Phase 2 and studying the effect of temperature variations on USW measurements.

6. References

Bertola, Numa, Philippe Schiltz, et al. “A Review of the Use of UHPFRC in Bridge Rehabilitation and New Construction in Switzerland.” *Frontiers in Built Environment*, vol. 7, 2021, p. 155.

Bertola, Numa, Ngoc Thanh Trinh, et al. “Experimental Investigation of a Keying Joint Cast in UHPFRC between Precast UHPFRC Bridge Elements.” *Materials and Structures*, vol. 55, no. 3, Mar. 2022, p. 86..

Brühwiler, Eugen. “UHPFRC Technology to Enhance the Performance of Existing Concrete Bridges.” *Structure and Infrastructure Engineering*, vol. 16, no. 1, Jan. 2020, pp. 94–105.

Brühwiler, Eugen, and Emmanuel Denarié. “Rehabilitation and Strengthening of Concrete Structures Using Ultra-High Performance Fibre Reinforced Concrete.” *Structural Engineering International*, vol. 23, no. 4, 4, Nov. 2013, pp. 450–57.

Graybeal, Benjamin, et al. “International Perspective on UHPC in Bridge Engineering.” *Journal of Bridge Engineering*, vol. 25, no. 11, Nov. 2020, p. 04020094.

Habel, Katrin, et al. “Development of the Mechanical Properties of an Ultra-High Performance Fiber Reinforced Concrete (UHPFRC).” *Cement and Concrete Research*, vol. 36, no. 7, 7, July 2006, pp. 1362–70.

Habel, Katrin, and Paul Gauvreau. “Response of Ultra-High Performance Fiber Reinforced Concrete (UHPFRC) to Impact and Static Loading.” *Cement and Concrete Composites*, vol. 30, no. 10, Nov. 2008, pp. 938–46.

Hajiesmaeili, Amir, and Emmanuel Denarié. “Capillary Flow in UHPFRC with Synthetic Fibers, under High Tensile Stresses.” *Cement and Concrete Research*, vol. 143, May 2021, p. 106368.

Kazemi Kamyab, Mohammadhadi. *Autogenous Shrinkage and Hydration Kinetics of SH-UHPFRC under Moderate to Low Temperature Curing Conditions*. EPFL, 2013.

Kazemi-Kamyab, Hadi, et al. “Kinetics of Mixing-Water Repartition in UHPFRC Paste and Its Effect on Hydration and Microstructural Development.” *Cement and Concrete Research*, vol. 124, Oct. 2019, p. 105784.

Kurz, Jochen H., et al. “Source Localization.” *Acoustic Emission Testing: Basics for Research – Applications in Engineering*, edited by Christian U. Grosse et al., Springer International Publishing, 2022, pp. 117–71.

Niederleithinger, Ernst, et al. “Embedded Ultrasonic Transducers for Active and Passive Concrete Monitoring.” *Sensors*, vol. 15, no. 5, 5, May 2015, pp. 9756–72.

Schumacher, Thomas, and Ernst Niederleithinger. “Combining Passive and Active Ultrasonic Stress Wave Monitoring Techniques: Opportunities for Condition Evaluation of Concrete Structures.” *NDT-CE 2022 - The International Symposium on Nondestructive Testing in Civil Engineering Zurich, Switzerland, August 16-18, 2022*, Aug. 2022,

Technical Leaflet on UHPFRC: Materials, Design and Application. 2016, p. 48.